https://doi.org/10.15255/KUI.2021.085
KUI-1/2023
Original scientific paper
Received December 20, 2021
Accepted July 31, 2022

Modelling and Multi-response Optimisation of Leachate Treatment by Electrocoagulation using Full Central Composite Design

R. Lessoued,[a] *A. Azizi*,[b*] *M. Lati*,[c] and *T. Ahmed Zaid*[d]

[a] Process Engineering Laboratory, University of Kasdi Merbah, Ouargla, PO Box 511, 30 000, Ouargla, Algeria
[b] Faculty of Technology, University Amar Telidji of Laghouat, Highway Ghardaia post box G37 (M'kam) 03 000, Laghouat, Algeria
[c] New and Renewable Energy Development Laboratory in Arid and Saharan Zones, University of Ouargla, 30 000, Ouargla, Algeria
[d] Laboratory of Fossil Energy Recovery, Chemical Engineering Department, Nationale Polytechnique School, El Harrach 16 200, Algiers, Algeria

Abstract

Electrocoagulation has lately received much interest as an effective method for the treatment of landfill leachate because of its ease of use, low cost, and environmental friendliness. The present study aimed to investigate the reduction of chemical organic demand (COD), biological organic demand (BOD_5), and turbidity from leachate by electrocoagulation process using aluminium electrodes. In order to achieve the maximum removal of pollutants, highlight the key effects of the variables and their simultaneous relationships, full central composite design was applied. Moreover, the backward model selection method using Bayesian Information Criterion and Akaike Information Criterion was carried out to determine the most suitable model with relevant effects. The optimum conditions indicated by the estimated quadratic models were initial pH (5.04), current density (407 A m^{-2}), reaction time (74.6 min), and stirring speed (150 rpm), adjusted R^2 of 99.82 %, 99.93 %, and 99.95 % for COD, BOD_5, and turbidity, respectively. Electrocoagulation was also successful in achieving 90 % COD, 92.3 % BOD_5, and 99.6 % turbidity removal efficiency. The findings indicated a satisfactory agreement between model forecasts and experimental values.

Keywords

Wastewater, electrocoagulation, backward selection, central composite design, response surface methodology

1 Introduction

Landfilling in most countries is currently the most common method for the disposal of municipal solid waste (DSM) due to its reduced functioning costs and simplicity of operations management.[1] Additionally, heterogeneous waste deposited in landfills undergoes many physicochemical reactions, resulting in a highly contaminated, dark, malodourous fluid called leachate, with noticeable variations in physicochemical characteristics and volumetric flow.[2] The decomposition, volume of leachate produced, stabilisation, and removal of contaminants from the waste matrix depends on several parameters, such as waste type, level of compaction, and waste absorption ability.[3] Leachate is typically highly contaminated with organic pollutants, expressed through colour, chemical organic demand (COD) and biological organic demand (BOD_5), and with content of ammonia, halogenated hydrocarbons, and heavy metals.[4] Unsuitable treatment of leachate causes environmental threats, in particular *via* the pollution of groundwater and surface water.[5] Leachate can be considered an intense wastewater pollutant, and must be adequately managed before being released to the receiving water bodies.[6] Currently, several treatment processes for landfill leachate can be used.[7] *Amr et al.*[8] have shown that biological treatment involves aerobic and anaerobic procedures, biological methods, as well as successful treatment of young leachates; meanwhile, physical and chemical treatments including a variety of techniques, such as coagulation-flocculation, adsorption, ion exchange, and oxidation, are further useful in treating stable leachates.[6] Efficient and economical methods for treating and reusing industrial wastewater have become an essential requirement for protection of the ecosystem.[9]

In recent years, electrocoagulation (EC) treatments are favoured as they are cost-effective and highly efficient for the treatment of municipal wastewater compared with other treatment techniques.[10] Among these techniques, EC has been commonly employed for the treatment of municipal wastewater,[11] urban wastewater,[12] surface water,[13] domestic wastewater,[14] industrial wastewater,[15] seawater,[16] and groundwater.[17] The advantages of this technique include environmental sustainability, flexibility, selectivity, energy efficiency, mechanisation capability, protection, and cost-effectiveness.[18] In general, an EC system comprises three important stages, i.e., coagulation, flotation, and electrochemistry.[19] EC often involves electrolysis, ionisation, hydrolysis, and free hydroxyl radical processes in landfill leachate treatment, which contribute to substantial variations in the aqueous medium compositions, as well as improvement in the overall removal of contaminants.[20] Besides the relatively low cost and ease of procurement of aluminium electrodes, several studies[21–23] have proven that these electrodes perform better with regard to various contaminants, such as organic, inorganic, and pathogenic, in the treatments of landfill leachate.[22,24,25] Moreover,

* Corresponding author: Assoc. Prof. Ahmed Azizi
Email: a.azizi@lagh-univ.dz

in the removal of dissolved organic pollutants assessed by colour, turbidity, and COD reduction, aluminium electrodes prove to be more effective compared to other types of electrodes.[26,27] At an adequate pH, organic compounds are removed by applying the required potential.[28,29] When the electric current begins to pass through the submerged electrodes, the cathode releases hydroxide ions (OH^-) and hydrogen gas (H_2), and the anode begins to dissolve and generate highly charged cations (Al^{3+}). At the surface of the anode, the contaminants are adsorbed and the colloidal particles destabilised by the formation of complex hydroxo-monomeric and polymeric aluminium species, which have high adsorption properties, forming strong aggregates with the pollutants that can be separated by filtration, flotation or sedimentation.[30–34]

Kobya et al.[35] stated that the efficacy of EC treatment is related to several specific operating criteria, like electrode material used, electrode distance, electrolyte concentration, initial pH, conductivity, reaction time, initial concentration of the pollutants, mixing speed, and current density.[36] Like any other processing technology, EC has some disadvantages that could affect its performance, i.e., high costs of electricity and generation of secondary pollutants.[37–38]

In many studies investigating wastewater treatment using conventional EC method, the authors proceeded by changing one variable at a time (OVAT) while keeping constant the other variables of the process.[39,40] This approach has the shortcoming of depending upon guesswork, chance, experience, and intuition. Furthermore, the procedure needs massive amounts of resources to obtain a limited number of method data. OVAT experiments are sometimes inaccurate, ineffective, and time-consuming, and can lead to incorrect optimum process conditions.[41] These limitations can be addressed by using response surface methodology (RSM), which allows several input variables to be varied at the same time while assessing their effects on several output responses.[41] RSM is a set of statistical tools and sequential experimentation strategies that are helpful in the development of analytical models and process optimisation.[42] By using RSM, adequate multi-response models can be generated and the operating parameters are easily optimised. As a sub-model of RSM, Central Composite Design (CCD) is a commonly applied experimental design which helps to build a second-order response surface model requiring fewer experimental sets, and to assess the effects of different input variables on the selected responses.[29,42]

In the present work, full central composite design (FCCD) with orthogonal backward elimination procedure (OEB) were performed to design experiments and maximise simultaneously the COD, BOD_5, and turbidity removal efficiency by EC treatment. In addition, analysis of variance (ANOVA) at significance level (SL) of 95 % was performed to select the significant coefficients and eliminate insignificant parameters from developed models. The main goals of the study were as follows:

- Reduction of EC process operating costs by restricting the number of experiments;
- Development of a mathematical model that can accurately predict the maximum removal of contaminants and optimise overall process efficiency.
- Provide a better understanding of the relationship between key process inputs and outputs.
- Assessment of the effects of four quantitative factors (reaction time, initial pH, current density, and stirring speed) on the responses under study (COD, BOD_5, and turbidity).
- Promote an environmentally friendly process for municipal wastewater treatment.

Materials and methods

2.1 Characterisation of leachate

The leachate for this study was collected from Laghouat city landfill (400 km south of the Algerian capital at coordinates 33°42′19″ N and 2°54′37″ E) in a closed plastic container, and stored in obscurity at $T = 4$ °C. All analyses were conducted in triplicate. BOD_5 was determined using the Warburg method (WTW, Expotech, USA), and COD was measured using the SpectroScan 80DV Visible-UV system (Biotech Co. Ltd., UK). Conductivity, turbidity, and pH measurements were achieved using a HANNA HI 8733 (HANNA instruments, India), WTW Turb 555 IR (Expotech, USA), and an Adwa AD 110 (*Adwa Instruments,* Hungary *Kft*.), respectively.

2.2 Experimental setup

EC studies were conducted at room temperature (28 °C) using an EC laboratory cell in batch mode with a total leachate sample volume of 400 ml. Electrodes were attached to a direct current (DC) power supply (PHYWE System GmbH & Co. KG, Germany, 0-2A, 0-12V), and a magnetic mixer (AREX, VELP Scientific Inc., USA) was used for gentle agitation. The reactor included aluminium (Al) electrodes ($0.3 \times 2.4 \times 6.1$ cm) coupled as anode and cathode in monopolar parallel mode. The overall effective area and electrode spacing was 34.5 cm^2 and 3.1 cm, respectively. The electrodes were submerged in HCl solution after each test run, and washed with deionised water. The variables studied were reaction time (x_1), pH (x_2), current density (x_3), and magnetic stirring speed (x_4). By adding an adequate amount of sodium hydroxide (NaOH) and hydrochloric acid (HCl) solutions (0.1 M), the pH of the measurements was adjusted to the targeted values. The supernatant was extracted and examined after 60 min of settling time.

2.3 Process modelling and data analysis

In this study, several regression models, including linear polynomial and Quadratic polynomial, were investigated. Full central composite design (FCCD) comprising 31 runs was applied to estimate the effects of major operational parameters, and to improve the removal efficiency of COD, BOD_5, and turbidity from leachate. In order to determine which significant terms must be retained in the empirical models, orthogonal backward elimination procedure (OEB) at 95 % SL was performed. This approach begins with all the variables involved in the model, and the variables are then excluded one at a time. For each level, the

variable that is omitted is the one that results in the lowest inflation in the residual sum of squares. This elimination proceeds until only one element is left in the model or until the stop rule is fulfilled.[43] Subsequently, ANOVA was conducted to define the most appropriate factors for the designated model. The experiments were conducted using the Minitab Software Trial (Version 19, Minitab Inc., State College, Pennsylvania). The defined values of the chosen variables (Table 1) are defined based on a significant number of tests. Each variable was coded at five levels.

Polynomial models of second order can be presented in accordance with Eq. (1) to forecast the best settings, and consider the relationship between the parameters.

$$Y = \beta_0 + \sum_{i=1}^{k} \beta_i x_i + \sum_{i=1}^{k} \sum_{j=i+1}^{k} \beta_{ij} x_i x_j + \sum_{i=1}^{k} \beta_{ii} x_i^2 + \varepsilon \quad (1)$$

where β_0 is the constant coefficient; β_i, β_{ij} and β_{ii} are the linear, interactive, and quadratic regression coefficients, respectively; k is the number of parameters; x_i and x_j are independent variables, and is the error term.[29]

Table 1 – Experimental range and levels of independent variables

Coded levels					
Variables	−1.414	−1	0	+1	+1.414
Actual levels					
Reaction time / min: X_1	24.55	32	50	68	75
Initial pH : X_2	3	3.6	5	6.40	6.98
Current density / A m^{-2}: X_3	241	291	407	523	573
Stirring speed / rpm: X_4	114	125	150	175	185.30

The overall performance of the fitted models was measured by the coefficient of determination (R^2), adjusted R^2 (R^2adj), and predicted R^2 (R^2pred). The R^2 coefficient was determined to check the fitting of the model. The closer the values of R^2 to 1, the stronger the model and the better the prediction of the response. For good fit of models, the coefficient of correlation (R^2) should be at least 80 %.[8]

The prediction error sum of squares (PRESS) was used to assess the predictive ability of models. Generally, the lower the PRESS value, the better the model predictive capability. Standard deviation S evaluates how well the responses are described by the model. Moreover, the Bayesian Information Criterion (BIC) and the Akaike Information Criterion (AICc) parameters were also used for comparison of several models. It is particularly appropriate when comparing mixed-effects of nonlinear models. Smaller values to these statistics are preferred.[44] Model terms were evaluated with 95 % confidence level. For small probability P-value, the corresponding model and the individual coefficient become more significant.[45] The data variation around the adjusted model is defined by the lack of fit. If the model matches the data correctly, the lack of fit must be higher than 0.05.[46]

The Pareto chart was used to measure the influence of the independent variables, as well as the relationship between them, in which any effects with an absolute value greater than 2.1 are considered significant. Statistically, the red line in the graph demonstrates the level of the low relevant term. Three-dimensional plots were illustrated, and depending on the key factors in the overlay graph, the optimum area was determined. Finally, to validate models, triplicate confirmatory tests were performed using the optimal conditions generated from statistical optimisation based on the high desirability that RSM implied. By comparing the experimental data and the expected results, the model's accuracy and suitability were assessed.

3 Results and discussion

3.1 Characteristics of the landfill wastewater

The main characteristics of the raw leachate, such as COD, BOD_5, conductivity, pH, and turbidity were analysed. Leachate was heavily polluted. It had a high pH value of approximately 8.1, a high turbidity of 283 NTU, and a substantial content of dissolved substances (conductivity of 33.1 mS cm^{-1}). Biodegradable organic matter reached concentrations of up to 1300 mgO_2 l^{-1}, and values of COD were around 20011 mgO_2 l^{-1}. Furthermore, leachate had a comparatively very low biodegradability ratio BOD_5: COD of 0.064 (< 0.1).

3.2 Statistical analysis, optimisation, and model validation

ANOVA was employed to examine the connection between input variables and COD (Y_1), BOD_5 (Y_2), and turbidity (Y_3) removal efficiencies for the EC process. In order to achieve an appropriate fit in a given model, significant model parameters are required. The FCCD provided in Table 2 permitted the generation of mathematical equations in which expected responses were related to the four factors (x_1, x_2, x_3 and x_4). Using coded factors, Eqs. (2–4) of the estimated models are as follows:

$$\begin{aligned} Y_1(\%) = {} & -98.57 - 0.073x_1 + 1.97x_2 + 0.3x_3 + 1.59x_4 - \\ & 0.0008x_1^2 - 0.75x_2^2 - 0.0004x_3^2 + 0.0047x_4^2 \\ & +0.09x_1x_2 - 0.0012x_1x_3 + 0.0016x_1x_4 + 0.013x_2x_3 - 0.037x_2x_4 \end{aligned} \quad (2)$$

$$\begin{aligned} Y_2(\%) = {} & -90.05 + 0.3x_1 + 3.034x_2 + 0.077x_3 + 1.88x_4 - 1.1x_2^2 \\ & -0.00016x_3^2 - 0.0082x_4^2 - 0.16x_1x_2 + 0.0001x_1x_3 \\ & +0.004x_1x_4 + 0.01x_2x_3 + 0.085x_2x_4 \end{aligned} \quad (3)$$

$$\begin{aligned} Y_3(\%) = {} & -125.55 - 0.91x_1 + 19.26x^2 + 0.267x_3 + 1.86x^4 - 3.75x^2{}_2 - 0.0003x_3^2 \\ & -0.0066x_4^2 + 0.22x_1x_2 - 0.001x_1x_3 + 0.0027x_1x_4 + 0.007x_2x_3 + 0.004x_2x_4 \end{aligned} \quad (4)$$

Fig. 1 shows the Pareto charts for COD, BOD_5, and turbidity removal. A grey bar indicates a term that is not included in the model. The key variables, x_1 (A), x_2 (B), x_3 (C), and x_4 (D) along with the interaction effect of the AC, AB, BC, BD, and AD extending outside the red line are statistically significant at 95 % confidence level. Fig. 1a shows that the coefficient CD (x_3x_4) was not significant on COD removal,

Table 2 – Results for COD, BOD_5, and turbidity reduction

Run No.	Experimental design				COD / %		BOD_5 / %		Turbidity / %	
	t	pH	*I*	*V*	Actual	Predicted	Actual	Predicted	Actual	Predicted
1	+1	−1	−1	−1	80.00	80.07	87.50	87.50	81.90	81.95
2	−1	+1	−1	−1	69.90	69.96	80.70	80.70	60.55	60.58
3	−1	−1	+1	−1	83.90	81.21	76.00	76.00	94.40	94.54
4	+1	+1	+1	−1	79.50	79.80	76.60	76.60	84.50	84.54
5	−1	−1	−1	+1	84.40	84.17	72.25	72.25	83.60	83.64
6	+1	+1	−1	+1	82.41	82.23	84.00	84.00	83.10	83.04
7	+1	−1	+1	+1	79.12	79.14	84.50	84.50	86.17	86.17
8	−1	+1	+1	+1	80.00	80.00	88.53	88.53	73.50	73.48
9	0	0	0	0	89.53	89.27	90.50	90.50	96.10	96.16
10	0	0	0	0	89.30	89.27	91.00	91.00	96.50	96.16
11	−1	−1	−1	−1	79.50	79.43	79.50	79.50	85.20	85.20
12	+1	+1	−1	−1	80.00	79.73	72.70	72.70	79.30	79.12
13	+1	−1	+1	−1	71.70	71.43	84.70	84.70	83.00	82.82
14	−1	+1	+1	−1	80.80	80.47	83.60	83.60	74.50	74.48
15	+1	−1	−1	+1	87.60	87.78	87.20	87.20	85.40	85.31
16	−1	+1	−1	+1	69.40	69.51	85.57	85.57	59.51	59.58
17	−1	−1	+1	+1	85.84	85.95	68.90	68.90	92.95	92.97
18	+1	+1	+1	+1	82.40	82.31	88.10	88.10	88.62	88.46
19	0	0	0	0	89.22	89.24	91.00	91.00	96.10	96.16
20	0	0	0	0	89.04	89.27	90.76	90.76	96.60	96.16
21	−α	0	0	0	87.72	87.73	87.70	87.70	92.00	92.02
22	+α	0	0	0	89.67	89.81	93.28	93.28	99.60	99.99
23	0	−α	0	0	88.65	88.55	84.60	84.60	89.37	89.35
24	0	+α	0	0	83.86	84.10	88.00	88.00	73.40	73.57
25	0	0	−α	0	78.15	78.34	86.00	86.00	83.30	83.36
26	0	0	+α	0	79.71	79.67	86.30	86.30	93.84	93.93
27	0	0	0	−α	80.67	80.80	78.80	78.80	87.00	87.04
28	0	0	0	+α	85.90	85.92	82.00	82.00	88.60	88.71
29	0	0	0	0	89.71	89.27	90.60	90.60	96.10	96.16
30	0	0	0	0	89.20	89.27	90.85	90.85	96.30	96.16
31	0	0	0	0	89.21	89.27	90.80	90.80	96.25	96.16

so it was not included in the estimated model. The quadratic effect of stirring speed (CC) had the largest influence on COD removal, as can be seen from Fig. 1a. Moreover, Figs. 1b and c show that the coefficients CD (x_3x_4) and AA (x_1x_1) were not significant on BOD_5 and turbidity removal, so they were excluded from the corresponding models. Reaction time (A) and initial pH (B) had the most substantial effect on BOD_5 and turbidity removal, respectively.

Normal probability plots were used to identify the actual effects (Fig. 2). Based on the normal probability graphs, the points placed along the adjusted line were not found to be important, although the points located far out of the line appear to be most important. All quadratic effects are important, and those represented with the blue triangle are irrelevant. As may be seen in Fig. 2, the key factors (*t*, pH, *I*, and *V*) are distant from the diagonal line and were therefore considered important.

Fig. 2a shows that the three variables, time (A), current density (C), and stirring speed (D) located on the right of the red line, had a positive effect on COD removal, while pH (B) on the left side had a negative effect. Since its point appears furthest from the line, quadratic effect current density*current density (CC) had the highest impact. The next major element was time*current density (AC). As far

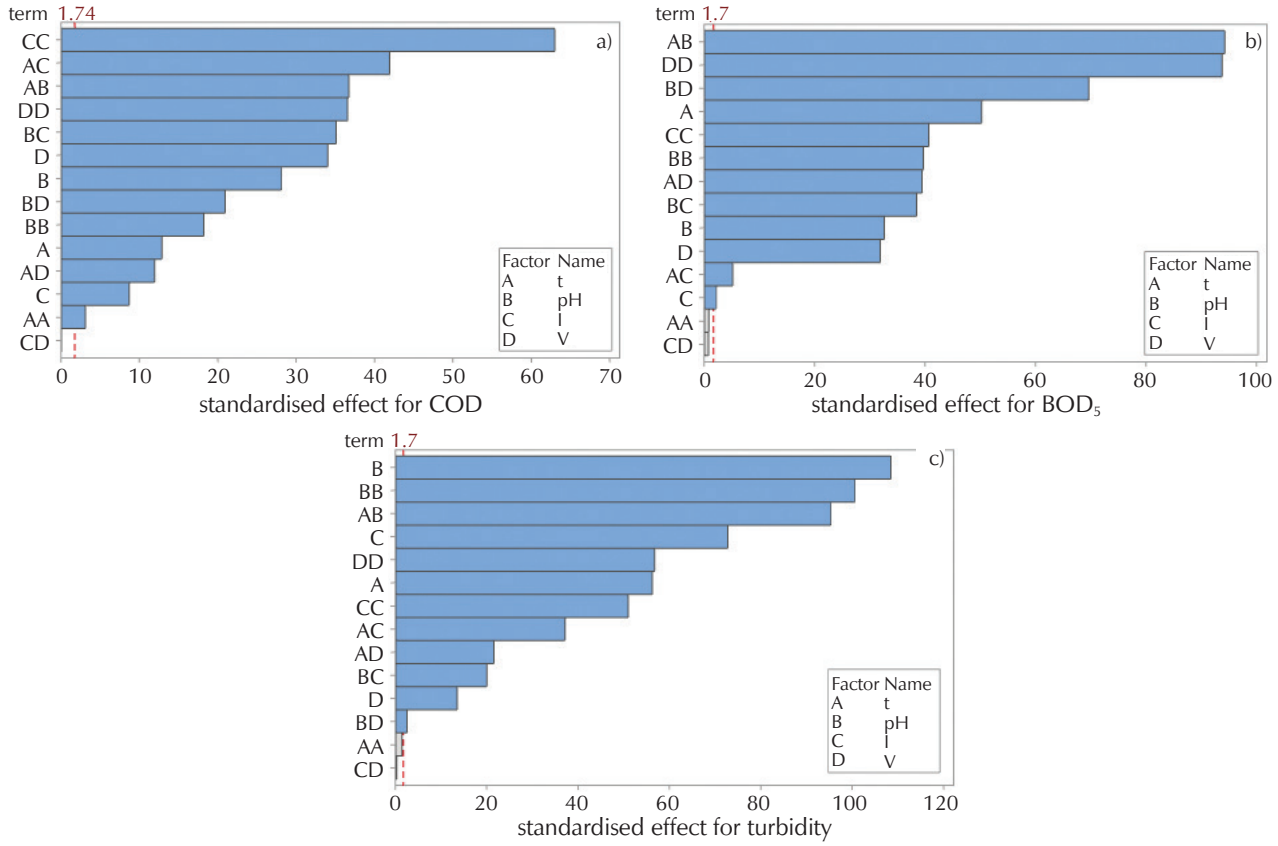

Fig. 1 – Pareto graph of standardised effects for (a) COD, (b) BOD_5, and (c) turbidity reduction

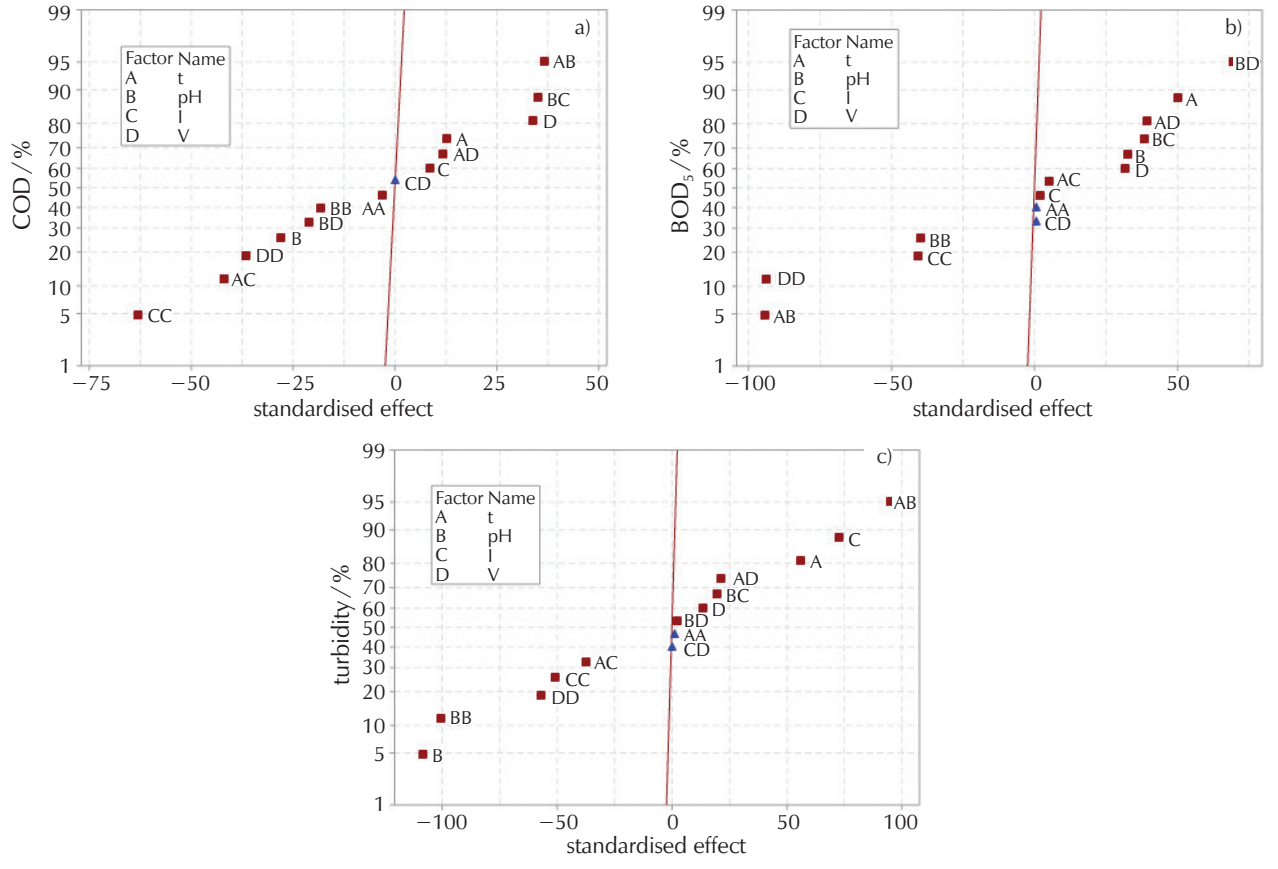

Fig. 2 – Normal probability graph for standardised effects of model variables for (a) COD, (b) BOD_5, and (c) turbidity reduction

as interacting terms are concerned, AC, AB, and BC had an important influence on the effectiveness of COD removal. Such interaction effects showed that the percentage of removal performance was higher at higher values of time, stirring speed, current density, and low pH.

From Fig. 2b, all the main factors: time reaction (*t*), pH, current density (*I*), and stirring speed (*V*) on the right had a positive effect on the BOD_5 removal. Fig. 2c shows that B on the left had a negative influence, whereas A, C, and D on the right had a positive impact on turbidity removal. The quadratic term pH*pH (BB) had the greatest effect.

The predicted *vs.* experimental values plots for the responses under study are shown in Fig. 3a–c. It may be seen that all the points are close to the diagonal line, implying good agreement between the experimental data and the expected output data of the model. The coefficient of correlation of 0.9922, 0.9996, and 0.9998 highlights the good reliability of the developed models for COD, BOD_5, and turbidity removal. Furthermore, a normal probability graph of residuals is considered to assess the validity of the models. As seen in Fig. 4a–c, the points in the normal probability plots of residuals for COD, BOD_5, and turbidity removal fit well in a straight line, so the residuals are normally distributed. Low dispersion of the points from the reference line indicates high quality of the models.

In order to assess the statistical importance of the regression coefficients, the analysis of variance (ANOVA) was performed for experimental results, presented in Table 3. The ANOVA of the regression model indicates that the model's terms are highly significant with a very low *P*-value (probability value < 0.05). As reported in Table 3, the R^2 values indicate that the models as fitted explain 99.90, 99.96, and 99.97 % of the COD, BOD_5 and turbidity variances, respectively. The adjusted R^2 (R^2adj) should be sufficiently close to R^2 value (R^2-R^2adj <5 %) to indicate that undesired input factors toned not be excluded from the equation.[47] The R^2adj values, which are more suitable to compare models with different numbers of independent variables, were 99.82, 99.93, and 99.95 % respectively. Predicted R^2 (R^2pred) defines how well the model predicts the output variables for a new set of data. R^2pred values should be consistent with R^2adj as an indicator of the regression model's predictive ability.[48] The larger the R^2pred, the more precise the predictability of the model (R^2-R^2pred < 0.2). For comparing models, the latter is more relevant than R^2adj as it is focused on observations that are not involved in the model.[49] The estimated values of R^2pred expected the developed model to explain about 99.59, 99.89 and 99.94 % for COD (Y_1), BOD_5 (Y_2), and turbidity (Y_3), respectively, of variability in forecasting new findings. In accordance with these criteria, the overall predictability appeared to be quite satisfactory compared with previous results presented in refs.[45,46].

The AICc and BIC values shown in Table 3 were applied to assess the accuracy of various models when employing the method of backward elimination.[44] Higher R^2 values and

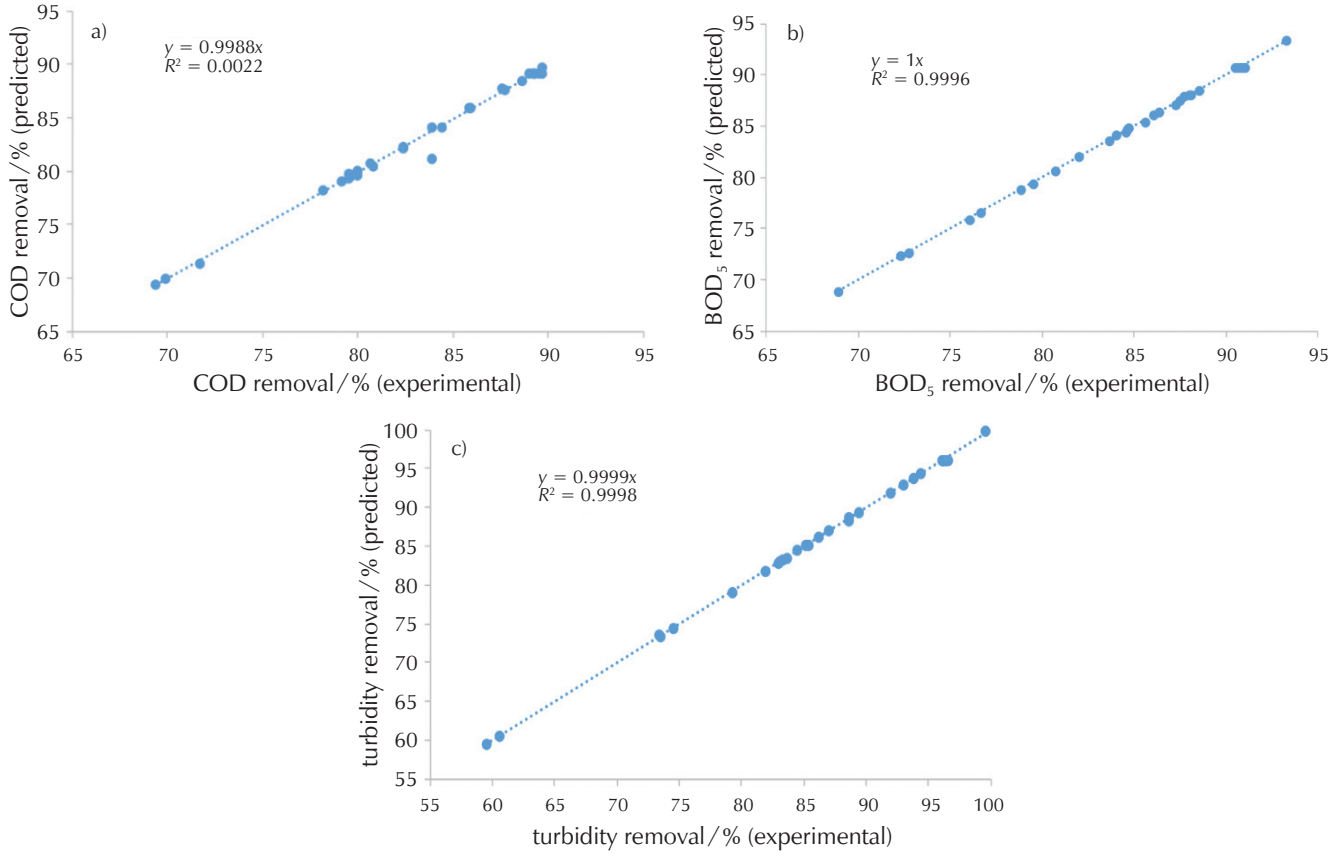

Fig. 3 – Experimental *vs.* predicted values plot for (a) COD, (b) BOD_5, and (c) turbidity removal

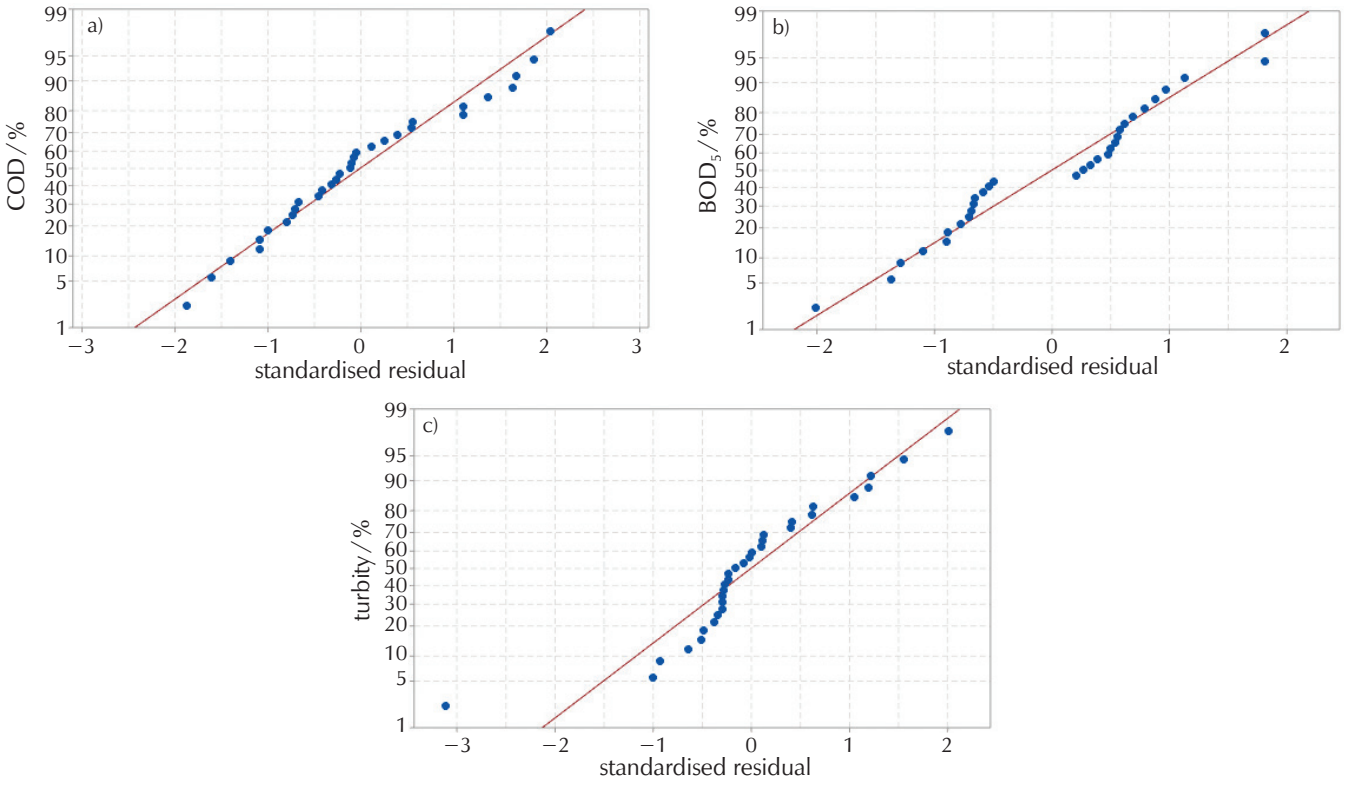

Fig. 4 – Normal probability plots of residuals for (a) COD, (b) BOD_5, and (c) turbidity removal

Table 3 – Models summary

Model	R^2(%)	R^2(*adj*) (%)	R^2(*pred*)(%)	PRESS	*S*	AICc	BIC	PLOF
COD	99.90	99.82	99.59	4.1473	0.2483	44.99	34.50	0.394
BOD_5	99.96	99.93	99.89	1.2679	0.1702	15.57	9.4	0.702
Turbidity	99.97	99.95	99.94	1.9831	0.2283	33.81	27.63	0.312

lower AICc and BIC values were identified, confirming that the fitted models can successfully estimate the removal of COD, BOD_5, and turbidity. The high *P*-values for lack of fit (PLOF) provided in the model summary table reveal that the *F*-statistics was insignificant, (PLOF > 0.05) confirming a strong model correlation between factors and model responses.

As revealed in Table 3, the standard deviation *S* of the data points all over the adjusted results were 0.24, 0.17, and 0.22, respectively. The multiple regression was restricted to reduce the expected error sum of squares (PRESS) for each individual process. The statistical analysis showed that the fitted quadratic models depicted in Eqs. (2–4) described fairly well the process under study. The fitness requirements for the quadratic equations as well as the alternative linear models were verified. The best description of data analysis for developed quadratic equations is reported in Table 3. The findings on R^2, R^2adj, R^2pred, PRESS, *S*, AICc, BIC, and PLOF showed that the quadratic polynomial models were adequately adjusted to establish a significant connection between the COD, BOD_5, and turbidity removal effectiveness and the influencing factors (*i.e.,* current density, time, stirring speed, and pH), and therefore to predict accurately the process outputs.

Three-dimensional (3D) surface plots of the COD, BOD_5, and turbidity removal were generated via the RSM equations. They indicate the effects and relationship of two predictor factors on the response, while the other two factors were kept unchanged within the experimental ranges. As shown in Figs. 5–7, the maximum removal of COD, BOD_5, and turbidity was found at a lower pH range between 4.5 and 6, and current density less than 523 $A\,m^{-2}$. The increase in COD and BOD_5 removal (Figs. 5 and 6) at this level of pH (acid medium) can be clarified by the transformation of Al^{3+} into soluble monomeric species such as $Al(OH)^{2+}$ and . By complex precipitation kinetics, these species are converted into insoluble $Al(OH)_3$ flocs. The generated amorphous $Al(OH)_3$ can absorb ions and even soluble organic compounds and/or trap colloidal particles, which then coagulate to form particles that precipitate, usually near neutral pH.[51] With these conditions, turbidity removal had also increased dramatically, as shown in Fig. 7. It was also

observed that the removal efficiency of pollutants had increased with increasing current density. At a higher current density, the amount of oxidised metal increased producing more hydroxide flocs to remove the contaminants. Moreover, the density of the bubbles increased and their size decreased with the increase in current density, which led to a considerable removal of contaminants, mainly: COD, BOD_5, and turbidity. In addition, an increase in current density increases the operating voltage and exacerbates the release of oxygen.[41,52] Therefore, for current density values above 523 $A\,m^{-2}$, a small irrelevant decline occurs. Therefore, it is suggested that the current density should be limited in order to avoid the development of excessive oxygen and remove other side effects such as heat generation.[53] Similar observations were obtained by *Holt et al.*[54] *Damaraju et al.*[55] found that charges tend to neutralise at lower pH levels as higher metal quantities are decomposed due to higher current density, leading to floc formation and increased removal efficiency. Furthermore, this result shows that the rate of removals is enhanced when electrolysis time and stirring speed increases at the same time, which enables a longer catalytic reaction time leading to an improvement in the degradation of contaminants and a larger amount of hydroxyl radicals, which allows the production of metal-polymer complex to further improve the removal percentage.[56]

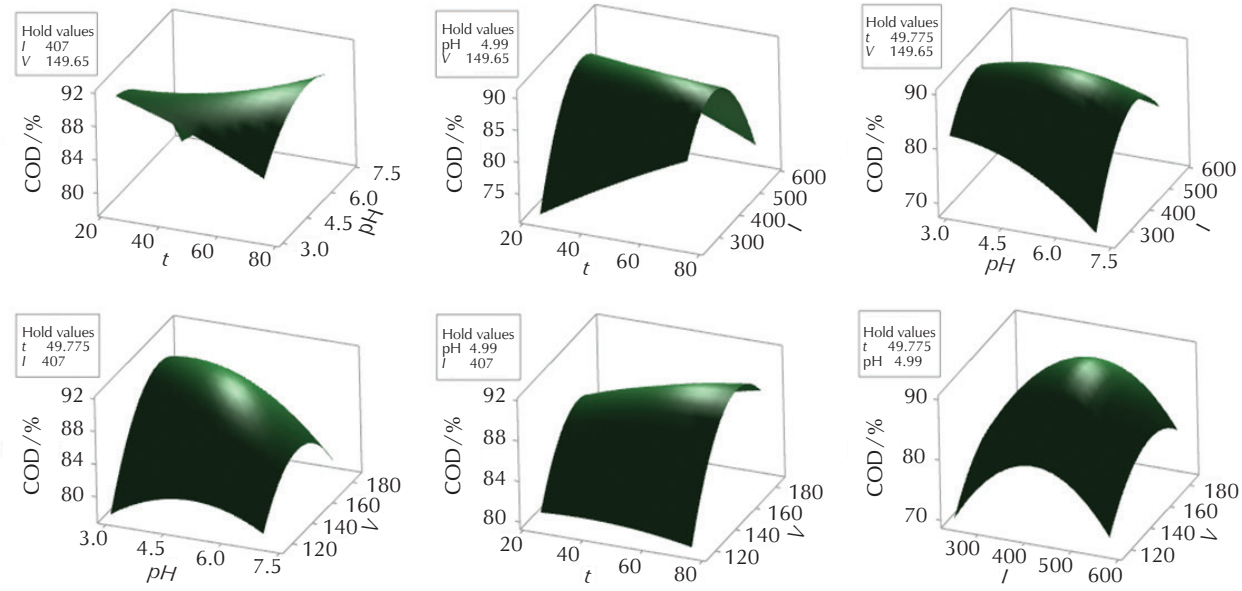

Fig. 5 – Three-dimensional response surface plots for the EC treatment of leachate for COD removal

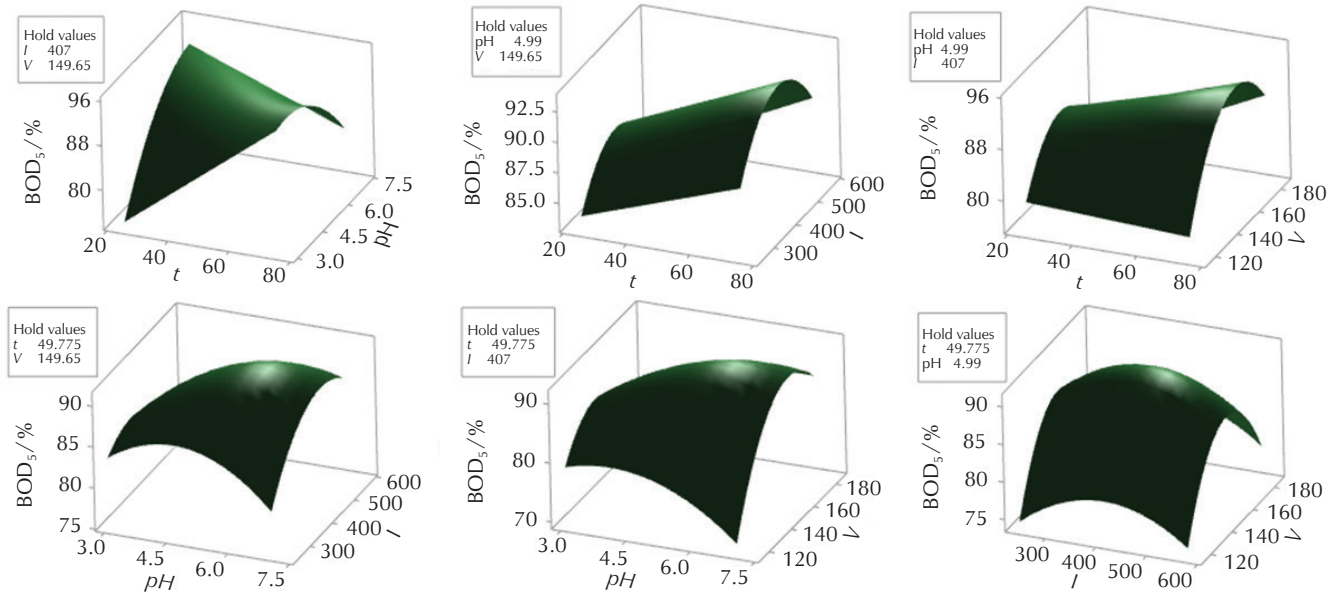

Fig. 6 – Three-dimensional response surface plots for the EC treatment of leachate for BOD_5 removal

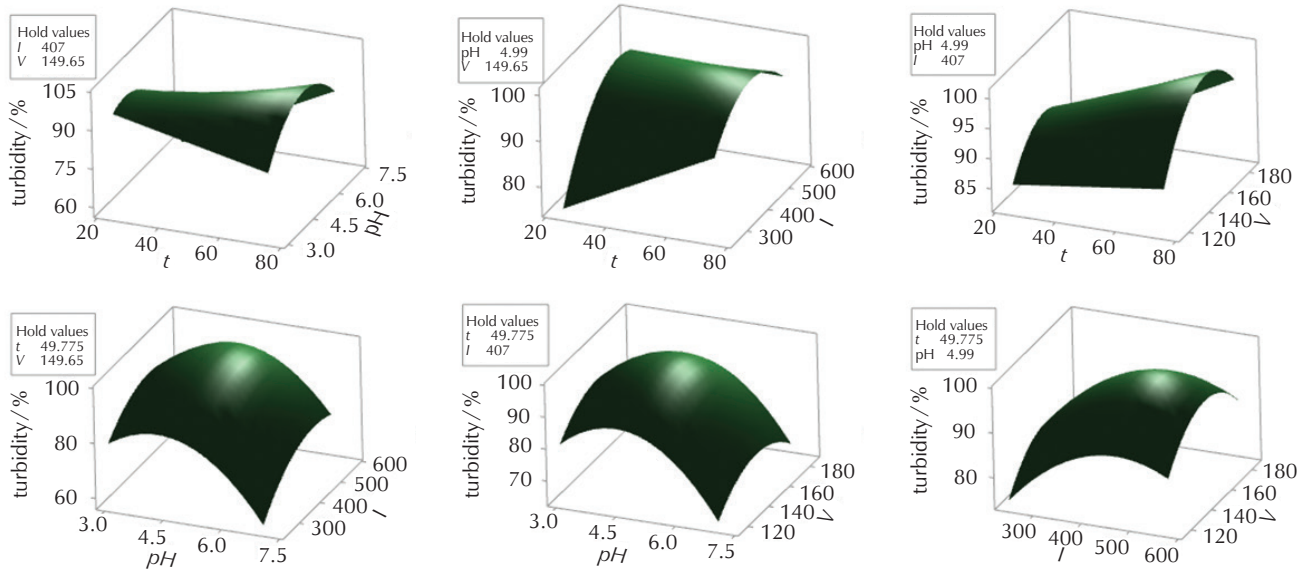

Fig. 7 – Three-dimensional response surface plots for the EC treatment of leachate for turbidity removal

Electrolysis time is another effective factor in the EC process. When the interaction effect between the initial pH and electrolysis time is examined, it is observed that the increase in electrocoagulation time increases the efficiency of COD, BOD_5, and turbidity removal. If the electrolysis time increases, the amount of aluminium hydroxide flocs increases. Namely, the formation of flocs in appropriate and sufficient quantities is time-dependent in the electrocoagulation process specifically, the formation of flocs in appropriate and sufficient quantities depends on the time of the EC process.[49]

Therefore, maximum removal rates higher than 89 % for COD, BOD_5, and turbidity were achieved within the current density range of 350–500 A m^{-2}, stirring speed of 140–160 rpm, pH of 4.5–6, and electrolysis time of 60–75 min.

Based on the surface response methodology and the desirability functions, numerical optimisation was conducted to determine the combination of optimal parametric settings, which concurrently increase COD, BOD_5, and turbidity removal.

The optimal operating values of all responses can also be defined by overlaying their shapes in an overlay plot wherein the optimum region against the grey zone, which did not follow the requirements, is clearly displayed in blank (Fig. 8).

The degree of desirability varied from 0 to 1, where zero (0) implies an unacceptable response, and one (1) is the most desired response.[57] A maximum composite desirability of 1 was reached. Tests were performed to check the optimum parameters. Validation tests were performed experimentally using the optimal values for each variable. Under these conditions (electrolysis duration of 74.6 min, pH of 5.04, current density of 407 A m^{-2}, and stirring speed of

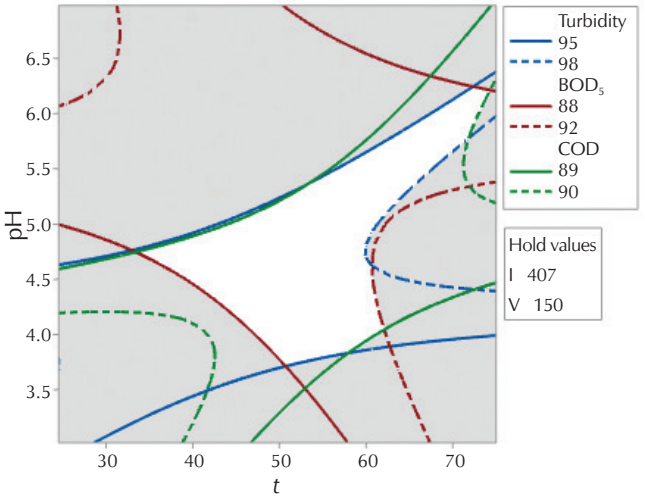

Fig. 8 – Overlay optimising graph for COD, BOD_5, and turbidity reduction

150 rpm), maximum removal efficiencies of 90 %, 92.3 %, and 99.6 % were obtained for COD, BOD_5, and turbidity removal, respectively. The actual value of COD, BOD_5, and turbidity removal shown in Table 4 were very close to those of the predicted results, which indicates that our models are good and reliable. Leachate is subject to clear black to light yellow discolouration following treatment.

Operating costs. The overall running costs were estimated using Eq. (5).

$$\text{operating cost} = a \cdot EN_C + B \cdot EL_C \qquad (5)$$

Table 4 – Confirmation experiments under optimum conditions

Response	Removal / %		Reaction time / min	pH	Current density/A m^{-2}	Stirring speed / rpm
	Predicted	Experimental				
COD	90.20	90	74.60	5.04	407	150
BOD_5	93.60	92.30				
Turbidity	100	99.60				

Table 5 – Comparison of recent studies on EC treatment of leachate using RSM methodology

Variables	Target response		Proposed model capability						Optimisation method	Ref.
Optimised conditions	*Y* Initial value	*R*/%	R^2/ %	R^2adj/%	R^2pred/%	PRESS	BIC	AICc		
t 60 min pH 8 *I* 30 mA cm^{-2}	COD 9800 mgO_2 l^{-1}	60.5	96	NA	NA	NA	NA	NA	RSM+ CCD	60
pH 7.73 *D* 1.16 cm NaCl 2 g l^{-1}	COD 7230 mgO_2 l^{-1} Colour 14750 ADMI	45.1 82.7	80.9 99.8	NA	NA	NA	NA	NA	RSM+ CCD	46
t 67.64 min pH 7.23 *I* 19.42 mA cm^{-2} *D* 0.96 cm	COD 840 mgO_2 l^{-1}	43	81	NA	NA	NA	NA	NA	RSM+ CCD	45
t 74.6 min pH 5.04 *I* 40 mA cm^{-2} *V* 150 rpm	COD **20011** mgO_2 l^{-1} BOD_5 **1300** mgO_2 l^{-1} Turbidity **283** NTU	**90** **92.3** **99.6**	99.9 99.9 99.9	99.8 99.9 99.9	99.6 99.8 99.9	4.14 1.27 1.98	34.5 9.4 27.6	44.9 15.6 33.8	RSM+FCCD+OEB+ +Responses verlaying	**Current study**

NA: not available; *Y*: Response; *R*: response reduction; R^2: determination coefficient; *Adj*R^2: adjusted R^2; *Pre*R^2: predicted R^2; BIC: Bayesian Information Criterion; AICc: Akaike Information Criterion; *D*: Inter-electrode distance; *V*: stirring speed; *I*: current density; *t*: electrolysis time. *OEB*: Orthogonal backward elimination procedure

The electrical energy consumption (EN_C) of the process and the aluminium electrode consumption (EL_C) can be calculated using Eqs. (6) and (7).[58]

$$EN_C = \frac{U \cdot i \cdot t}{V} \quad (6)$$

$$EL_C = \frac{i \cdot t \cdot M_w}{Z_{Al} \cdot F \cdot V} \quad (7)$$

where *U* is the applied voltage (V), *I* is the current (A), *t* is the *EC* reaction time (s), and *V* is the volume of leachate tested (m^3), M_w is the molecular mass of the aluminium electrode (26.98 g mol^{-1}), *F* is Faraday's constant (96487 C mol^{-1}), *Z* is the number of electrons transferred (Z_{Al} = 3), *a* is electrical energy price (0.014 US$ kW^{-1} h^{-1}, according to the Algerian market in April 2020), and *b* is electrode material price (1.6 US$ kg^{-1} Al^{-1}). The dissolved amount of electrodes was determined experimentally by calculating the difference between the sacrificial anode before and after each trial.[59] The power consumption and average dissolved mass of the anode were about 52 kwh m^{-3} and 0.13 g l^{-1}, respectively. The estimated operating cost of COD, BOD_5, and turbidity removal from leachate by *EC* process at optimum conditions was calculated to be 0.76 US$ m^{-3} leachate, which shows the viability of treatment of landfill leachates.

The findings of EC process efficiency and optimum operating conditions for leachate treatment observed in peer-reviewed literature and the current study are given in Table 5. As foreseen, these results demonstrate the good reproducibility of the proposed model in the design range.

4 Conclusions

In this research, FCCD with orthogonal backward elimination procedure (OEB) was applied to define optimum experimental parameters for EC leachate treatment, and to examine the effects of linear, interactive, and quadratic variables (pH, current density, stirring speed, and EC reaction time) on studied responses. Developed model results indicated a suitable relationship between experimental and expected values. ANOVA revealed a high coefficient of determination value (R^2 > 95 %), indicating a reasonable adjustment of the quadratic regression equation with the actual results. Under optimal operational factor settings of electrolysis duration 74.6 min, pH 5.04, current density 407 A m^{-2}, and stirring speed 150 rpm, the removal

efficiencies of COD, BOD_5, and turbidity from leachate reached 90 %, 92.3 % and 99.6 %, respectively. The findings showed that RSM and OEB were successfully exploited to optimise the operating parameters of EC treatment using small dissolved amounts of aluminium electrodes, at low operating cost of about 0.76 USD/m^3 of leachate treated.

List of abbreviations and symbols

AICc – Akaike information criterion
BIC – Bayesian information criterion
BOD_5 – biological organic demand
CCD – central composite design
COD – chemical organic demand
D – inter-electrode distance
DC – direct current
DSM – disposal of municipal solid waste
EC – electrocoagulation
FCCD – full central composite design
I – current density
LOF – lack of fit
NA – not available
OEB – orthogonal backward elimination procedure
OVAT – one variable at a time
PLOF – *P*-values for lack of fit
PRESS – prediction error sum of squares
R^2 – coefficient of determination
R^2adj – adjusted R^2
R^2pred – predicted R^2
RSM – response surface methodology
SL – significance level
t – electrolysis time
V – stirring speed
Y – response

References
Literatura

1. *A. Aziz, N. A. Rahim, S. F. Ramli, M. Y. Alazaiza, F. M. Omar, Y. T. Hung*, Potential use of Dimocarpus longan seeds as a flocculant in landfill leachate treatment, Water. **10** (11) (2018) 1672, doi: https://doi.org/10.3390/w10111672.
2. *Y. Peng,* Perspectives on technology for landfill leachate treatment, Arab. J. Chem. **10** (2017) S2567-S2574, doi: https://doi.org/10.1016/j.arabjc.2013.09.031.
3. *S. Mohan, R. Gandhimathi,* Removal of heavy metal ions from municipal solid waste leachate using coal fly ash as an adsorbent, J. Hazard. Mater. **169** (1-3) (2009) 351–359, doi: https://doi.org/10.1016/j.jhazmat.2009.03.104.
4. *K. H. Kang, H. S. Shin, H. Park,* Characterization of humic substances present in landfill leachates with different landfill ages and its implications, Water Res. **36** (16) (2002) 4023–4032, doi: https://doi.org/10.1016/S0043-1354(02)00114-8.
5. *S. K. Maiti, S. De, T. Hazra, A. Debsarkar, A. Dutta,* Characterization of leachate and its impact on surface and groundwater quality of a closed dumpsite – a case study at Dhapa, Kolkata, India. Procedia Environ. Sci. **35** (2016) 391–399, doi: https://doi.org/10.1016/j.proenv.2016.07.019.
6. *A. A. Hamid, H. A. Aziz, M. S. Yusoff S. A. Rezan,* Optimization and Analysis of Zeolite Augmented Electrocoagulation Process in the Reduction of High-Strength Ammonia in Saline Landfill Leachate. Water **12** (1) (2020) 247, doi: https://doi.org/10.3390/w12010247.
7. *A. Fernandes, M. J. Pacheco, L.Ciríaco, A. Lopes*. Review on the electrochemical processes for the treatment of sanitary landfill leachates: Present and future, Appl. Catal. B Environ. 176-177 (2015) 183–200, doi: https://doi.org/10.1016/j.apcatb.2015.03.052.
8. *S. S. A. Amr, H. A. Aziz, M. J. Bashir,* Application of response surface methodology (RSM) for optimization of semi-aerobic landfill leachate treatment using ozone, Appl. Water Sci. **4** (3) (2014) 231–239, doi: https://doi.org/10.1007/s13201-014-0156-z.
9. *G. Varank, S. Yazici Guvenc, G. Gurbuz, G. Onkal Engin,* Statistical optimization of process parameters for tannery wastewater treatment by electrocoagulation and electro-Fenton techniques, Desalin. Water Treat. **57** (53) (2016) 25460–25473, doi: https://doi.org/10.1080/19443994.2016.1157042.
10. *M. Van Genuchten, K. N. Dalby, M. Ceccato, S. L. S. Stipp, K. Dideriksen,* Factors affecting the Faradaic efficiency of Fe (0) electrocoagulation, J. Environ. Chem. Eng. **5** (5) (2017) 4958–4968, doi: https://doi.org/10.1016/j.jece.2017.09.008.
11. *M. B. Ensano, L. Borea, V. Naddeo, V. Belgiorno, M. D. G. De Luna, M. Balakrishnan, F. C. Ballesteros*, Applicability of the electrocoagulation process in treating real municipal wastewater containing pharmaceutical active compounds, J. Hazard. Mater. **361** (2019) 367–373, doi: https://doi.org/10.1016/j.jhazmat.2018.07.093.
12. *M. Elazzouzi, K. Haboubi, M. S. Elyoubi,* Enhancement of electrocoagulation-flotation process for urban wastewater treatment using Al and Fe electrodes: techno-economic study, Mater. Today, Proceedings **13** (2019) 549–555, doi: https://doi.org/10.1016/j.matpr.2019.04.012.
13. *K. S. Hashim, P. Kota, S. L. Z., R. Alwash, R. Al Khaddara, A. Shaw, D. Al-Jumeily, M. H. Aljefery,* Energy efficient electrocoagulation using baffle-plates electrodes for efficient *Escherichia coli* removal from wastewater, J. Water Process Eng. **33** (2020) 101079, doi: https://doi.org/10.1016/j.jwpe.2019.101079.
14. *P. I. Omwene, M. Kobya,* Treatment of domestic wastewater phosphate by electrocoagulation using Fe and Al electrodes: a comparative study, Process Saf. Environ. Prot. **116** (2018) 34–51, doi: https://doi.org/10.1016/j.psep.2018.01.005.
15. *J. W. Feng, Y. B. Sun, Z. Zheng, J. B. Zhang, S. Li, Y. C. Tian,* Treatment of tannery wastewater by electrocoagulation, J. Environ. Sci. **19** (12) (2007) 1409–1415, doi: https://doi.org/10.1016/S1001-0742(07)60230-7.
16. *X. Zhang, M. Lu, M. A. M. Idrus, C. Crombie, V. Jegatheesan,* Performance of precipitation and electrocoagulation as pretreatment of silica removal in brackish water and seawater, Process Saf. Environ. Prot. **126** (2019) 18–24, doi: https://doi.org/10.1016/j.psep.2019.03.024.
17. *M. A. Sandoval, R. Fuentes, J. L. Nava, O. Coreño, Y. Li, J. H. Hernández,* Simultaneous removal of fluoride and arsenic from groundwater by electrocoagulation using a filter-press flow reactor with a three-cell stack, Sep. Purif. Technol.

208 (2019) 208–216, doi: https://doi.org/10.1016/j.seppur.2018.02.018.

18. *J. N. Hakizimana, B. Gourich, M. Chafi, Y. Stiriba, C. Vial, P. Drogui, J. Naja,* Electrocoagulation process in water treatment: A review of electrocoagulation modeling approaches, Desalination **404** (2017) 1–21, doi: https://doi.org/10.1016/j.desal.2016.10.011.
19. *K. K. Garg, B. Prasad,* Treatment of multicomponent aqueous solution of purified terephthalic acid wastewater by electrocoagulation process: optimization of process and analysis of sludge, J. Taiwan Inst. Chem. Eng. **60** (2016) 383–393, doi: https://doi.org/10.1016/j.jtice.2015.10.038.
20. *Hassani, A. Alinejad, A. Sadat, A. Esmaeili, M. Ziaei, A. A. Bazrafshan, T. Sadat,* Optimization of landfill leachate treatment process by electrocoagulation, electroflotation and sedimentation sequential method, Int. J. Electrochem. Sci. **11** (2016) 6705–6718, doi: https://doi.org/10.20964/2016.08.10.
21. *A. Flilissa, P. Méléard, A. Darchen,* Selective removal of dodecyl sulfate during electrolysis with aluminum electrodes, Desalin. Water Treat. **51** (34-36) (2013) 6719–6728, doi: https://doi.org/10.1080/19443994.2013.769915.
22. *S. R. Tchamango, O. Kamdoum, D. Donfack, D. Babale,* Comparison of electrocoagulation and chemical coagulation processes in the treatment of an effluent of a textile factory, J. Appl. Sci. Environ. Manag. **21** (7) (2017) 1317–1322, doi: https://doi.org/10.4314/jasem.v21i7.17.
23. *L. W. M. Zailani, N. S. M. Zin,* Application of Electrocoagulation in wastewater treatment: A general review, IOP Conf. Ser., Earth Environ. Sci. **140** (2018) 012052, doi: https://doi.org/10.1088/1755-1315/140/1/012052.
24. *C. Barrera-Daz, B. Bilyeu, G. Roa, L. Bernal-Martinez,* Physicochemical Aspects of Electrocoagulation, Sep. Purif. Rev. **40** (1) (2011) 1–24, doi: https://doi.org/10.1080/15422119.2011.542737.
25. *J. Heffron, D. R. Ryan, B. K. Mayer,* Sequential electrocoagulation-electrooxidation for virus mitigation in drinking water, Water Res. **160** (2019) 435–444, doi: https://doi.org/10.1016/j.watres.2019.05.078.
26. *M. K. N. Mahmad, M. R. M. A. Z. Rozainy, I. Abustan, N. Baharun,* Electrocoagulation process by using aluminium and stainless-steel electrodes to treat total chromium, colour and turbidity, Procedia Chem. **19** (2016) 681–686, doi: https://doi.org/10.1016/j.proche.2016.03.070.
27. *P. Asaithambi, D. Beyene, A. R. A. Aziz, E. Alemayehu,* Removal of pollutants with determination of power consumption from landfill leachate wastewater using an electrocoagulation process: optimization using response surface methodology (RSM), Appl. Water Sci. **8** (2) (2018) 69, doi: https://doi.org/https://doi.org/10.1007/s13201-018-0715-9.
28. *D. Rajkumar, K. Palanivelu,* Electrochemical degradation of cresols for wastewater treatment, Ind. Eng. Chem. Res. **42** (9) (2003) 1833–1839, doi: https://doi.org/10.1021/ie020759e.
29. *G. Varank, S. Yazici, A. Demir, N. Kavan, N. Donmez, Z. T. Onen,* Modeling and optimizing electro-persulfate processes using Fe and Al electrodes for paper industry wastewater treatment, Water Sci. Technol. **81** (2) (2020) 345–357, doi: https://doi.org/10.2166/wst.2020.115.
30. *I. Kabdaşlı, I. Arslan-Alaton, T. Ölmez-Hancı, O. Tünay,* Electrocoagulation applications for industrial wastewaters: a critical review, Environ. Technol. Rev. **1** (1) (2012) 2–45, doi: https://doi.org/10.1080/21622515.2012.715390.
31. *M. Mechelhoff, G. H. Kelsall, N. J. Graham,* Electrochemical behavior of aluminum in electrocoagulation processes, Chem. Eng. Sci. **95** (2013) 301–312, doi: https://doi.org/10.1016/j.ces.2013.03.010.
32. *S. Garcia-Segura, M. M. S. G. Eiband, J. V. De Melo, C. A. Martínez-Huitle,* Electrocoagulation and advanced electrocoagulation processes: A general review about the fundamentals, emerging applications and its association with other technologies, J. Electro. Anal. Chem. **801** (2017) 267–299, doi: https://doi.org/10.1016/j.jelechem.2017.07.047.
33. *N. Galvão, J. B. De Souza, C. M. De Sousa Vidal,* Landfill leachate treatment by electrocoagulation: Effects of current density and electrolysis time, J. Environ. Chem. Eng. **8** (5) (2020) 104368, doi: https://doi.org/10.1016/j.jece.2020.104368.
34. *M. Ingelsson, N. Yasri, E. P. Roberts,* Electrode Passivation, Faradaic Efficiency, and Performance Enhancement Strategies in Electrocoagulation – A Review, Water Res. **187** (2020) 116433, doi: https://doi.org/10.1016/j.watres.2020.116433.
35. *M. Kobya, R. D. C. Soltani, P. I. Omwene, A. Khataee,* A review on decontamination of arsenic-contained water by electrocoagulation: Reactor configurations and operating cost along with removal mechanisms, Environ, Technol. Innov. **17** (2020) 100519, doi: https://doi.org/10.1016/j.eti.2019.100519.
36. *I. Sirés, E. Brillas,* Remediation of water pollution caused by pharmaceutical residues based on electrochemical separation and degradation technologies: a review, Environ. Int. **40** (2012) 212–229, doi: https://doi.org/10.1016/j.envint.2011.07.012.
37. *E. Mansour, E. S. Negim, I. H. Hasieb, O. A. Desouky, R. Abdykalykova, M. Beisebekov,* Removal of cadmium pollutants in drinking water using alternating current electrocoagulation technique, Glob. J. Environ. Res. **7** (2013) 45–51, doi: https://doi.org/10.5829/idosi.gjer. 2013.7.3.1102.
38. *E. Butler, Y. T. Hung, R. Y. L. Yeh, M. Suleiman Al Ahmad,* Electrocoagulation in wastewater treatment, Water **3** (2) (2011) 495–525, doi: https://doi.org/10.3390/w3020495.
39. *K. Sharma, A. K. Chopra,* Removal of nitrate and sulphate from biologically treated municipal wastewater by electrocoagulation, Appl. Water Sci. **7** (3) (2017) 1239–1246, doi: https://doi.org/10.1007/s13201-015-0320-0.
40. *M. Afsharnia, H. Biglari, S. S. Rasouli, A. Karimi, M. Kianmehr,* Sono-electrocoagulation of fresh leachate from municipal solid waste; simultaneous applying of iron and copper electrodes, Int. J. Electrochem. Sci. **13** (2018) 472–484, doi: https://doi.org/10.20964/2018.01.22.
41. *Y. Tak, B. S. Tak, Y. J. Kim, Y. J. Park, Y. H. Yoon, G. H. Min,* Optimization of color and COD removal from livestock wastewater by electrocoagulation process: application of Box–Behnken design (BBD), J. Ind. Eng. Chem. **28** (2015) 307–315, doi: https://doi.org/10.1016/j.jiec.2015.03.008.
42. *S. Karimifard, M. R. A. Moghaddam,* Application of response surface methodology in physicochemical removal of dyes from wastewater: a critical review, Sci. Total Environ. **640** (2018) 772–797, doi: https://doi.org/10.1016/j.scitotenv.2018.05.355.
43. *A. Akbarzadeh, M. Sadeghi,* Parameter study in plastic injection molding process using statistical methods and IWO algorithm, Int. J. Model. Optim. **1** (2) (2011) 141, doi: https://doi.org/10.7763/IJMO.2011.V1.25.
44. *B. Prajapati, R. Singh,* Enhancement of biogas production in bio-electrochemical digester from agricultural waste mixed with wastewater, Renew. Energy. **146** (2020) 460–468, doi: https://doi.org/10.1016/j.renene.2019.06.154.
45. *A. Ogedey, M. Tanyol,* optimizing electrocoagulation process using experimental design for COD removal from unsanitary landfill leachate, Water Sci. Technol. **76** (11) (2017) 2907–2917, doi: https://doi.org/10.2166/wst.2017.460.
46. *N. Huda, A. A. A. Raman, M. M. Bello, S. Ramesh,* Electrocoagulation treatment of raw landfill leachate using iron-based

electrodes: effects of process parameters and optimization, J. Environ. Manage. **204** (2017) 75–81, doi: https://doi.org/10.1016/j.jenvman.2017.08.028.

47. *A. Salarian, Z. Hami, N. Mirzaei, S. M. Mohseni, A. Asadi, H. Bahrami, M. R. Zare,* N-doped TiO_2 nanosheets for photocatalytic degradation and mineralization of diazinon under simulated solar irradiation: Optimization and modeling using a response surface methodology, J. Mol. Liq. **220** (2016) 183–191, doi: https://doi.org/10.1016/j.molliq.2016.04.060.
48. *M. Kobya, E. Demirbas, M. Bayramoglu, M. T. Sensoy,* Optimization of electrocoagulation process for the treatment of metal cutting wastewaters with response surface methodology, Water Air Soil Pollut. **215** (1-4) (2011) 399–410, doi: https://doi.org/10.1007/s11270-010-0486-x.
49. *Z. Beiramzadeh, M. Baqersad, M. Aghababaei,* Application of the response surface methodology (RSM) in heavy metal removal from real power plant wastewater using electrocoagulation, Eur. J. Environ. Civ. En. **26** (2022) 1–20, doi: https://doi.org/10.1080/19648189.2019.1640139.
50. *H. Kermet-Said, N. Moulai-Mostefa,* Optimization of Turbidity and COD Removal from Pharmaceutical Wastewater by Electrocoagulation. Isotherm Model. Cost Anal. Pol. J. Environ. Stud. **24** (3) (2015) 1049–1061, doi: https://doi.org/10.15244/pjoes/32334.
51. *K. Thirugnanasambandham, V. Sivakumar, P. J. Maran,* Efficiency of electrocoagulation method to treat chicken processing industry wastewater-modeling and optimization, J. Taiwan Inst. Chem. Eng. **45** (2014) 2427–2435, doi: https://doi.org/10.1016/j.jtice.2014.04.011.
52. *R. Katal, H. Pahlavanzadeh,* Influence of different combinations of aluminum and iron electrode on electrocoagulation efficiency: application to the treatment of paper mill wastewater, Desalination **265** (3) (2011) 199–205, doi: https://doi.org/10.1016/j.desal.2010.07.052.
53. *H. Holt, G. W. Barton, M. Wark, A. A. Mitchell,* A quantitative comparison between chemical dosing and electrocoagulation, Colloid Surf. A-Physicochem. Eng. Asp. **211** (2002) 233–248, doi: https://doi.org/10.1016/S0927-7757(02)00285-6.
54. *F. Hanafi, O. Assobhei, M. Mountadar,* Detoxification and discoloration of Moroccan olive mill wastewater by electrocoagulation, J. Hazard. Mater. **174** (2010) 807–812, doi: https://doi.org/10.1016/j.jhazmat.2009.09.124.
55. *M. Damaraju, D. Bhattacharyya, T. Panda, K. K. Kurilla,* Application of a Continuous Bipolar Mode Electrocoagulation (CBME) system for polishing distillery wastewater, E3S Web Conf. **93** (2019) 02005, doi: https://doi.org/10.1051/e3sconf/20199302005.
56. *S. U. Khan, D. T. Islam, I. H. Farooqi, S. Ayub, F. Basheer,* Hexavalent chromium removal in an electrocoagulation column reactor: Process optimization using CCD, adsorption kinetics and pH modulated sludge formation, Process Saf. Environ. Prot. **122** (2019) 118–130, doi: https://doi.org/10.1016/j.psep.2018.11.024.
57. *A. Bezerra, R. E. Santelli, E. P. Oliveira, L. S. Villar, L. A. Escaleira,* Response surface methodology (RSM) as a tool for optimization in analytical chemistry, Talanta. **76** (5) (2008) 965–977, doi: https://doi.org/10.1016/j.talanta.2008.05.019
58. *A. Hooshmandfar, B. Ayati, A. Khodadadi Darban,* Optimization of material and energy consumption for removal of Acid Red 14 by simultaneous electrocoagulation and electroflotation, Water Sci. Technol. **73** (1) (2016) 192–202, doi: https://doi.org/10.2166/wst.2015.477.
59. *K. S. Hashim, P. Kot, S. L. Zubaidi, R. Alwash, R. Al Khaddar, A. Shaw, D. Al-Jumeily, M. H. Aljefery,* Energy efficient electrocoagulation using baffle-plates electrodes for efficient, J. Water Process Eng. **33** (2020) 101079, doi: https://doi.org/10.1016/j.jwpe.2019.101079.
60. *H. A. Kabuk, F. Ilhan, Y. Avsar, U. Kurt, O. Apaydin, M. T. Gonullu,* Investigation of Leachate Treatment with Electrocoagulation and Optimization by Response Surface Methodology, Clean Soil Air Water **42** (2014) 571–577, doi: https://doi.org/10.1002/clen.201300086.

SAŽETAK

Modeliranje i optimizacija elektrokoagulacijske obrade procjednih voda uz primjenu centralno složenog plana eksperimenta

Ridha Lessoued,[a] *Ahmet Azizi*,[b*] *Moukhtar Lati* [c] i *Toudert Ahmed Zaid* [d]

Za obradu procjednih voda odlagališta otpada u posljednje se vrijeme sve više primjenjuje elektrokoagulacija. Razloga je više: od jednostavnosti primjene, niske cijene, visoke učinkovitosti do prihvatljivosti po okoliš. Cilj ovog istraživanja bio je ispitati učinkovitost obrade procjednih voda primjenom elektrokoagulacije pomoću aluminijskih elektroda. Pritom se pratila promjena koncentracije ukupne organske tvari izražena preko kemijske potrošnje kisika (KPK), biološke potrošnje kisika (BPK_5) i zamućenja. Da bi se postiglo maksimalno uklanjanje onečišćujućih tvari, istaknuli su se ključni učinci varijabli te ispitala simultanost njihovih odnosa, primijenjen je centralno složen plan eksperimenta. Optimalni uvjeti procijenjeni su kvadratnim modelima visokih vrijednosti prilagođenih koeficijenata determinacije od 99,82, 99,93 i 99,95 % za KPK, BPK_5, odnosno zamućenost. Optimalni uvjeti uključivali su početnu pH vrijednost od 5,04, gustoću struje od 407 A m^{-2}, reakciju u trajanju od 74,6 min te brzinu miješanja od 150 o min^{-1}. Elektrokoagulacijom postignuto je učinkovito uklanjanje organske tvari uz smanjenje KPK za 90 %, BPK_5 za 92,3 %, te zamućenja za 99,6 %. Rezultati su pokazali dobru podudarnost predviđenih i eksperimentalnih vrijednosti.

Ključne riječi
Otpadna voda, elektrokoagulacija, povratni odabir, centralno složeni plan eksperimenta, metodologija odzivne površine

[a] *Process Engineering Laboratory, University of Kasdi Merbah, Ouargla, PO Box 511, 30 000, Ouargla, Alžir*
[b] *Faculty of Technology, University Amar Telidji of Laghouat, Highway Ghardaia post box G37 (M'kam) 03000, Laghouat, Alžir*
[c] *New and Renewable Energy Development Laboratory in Arid and Saharan Zones, University of Ouargla, 30 000, Ouargla, Alžir*
[d] *Laboratory of Fossil Energy Recovery, Chemical Engineering Department, Nationale Polytechnique School, El Harrach 16200, Algiers, Alžir*

Izvorni znanstveni rad
Prispjelo 20. prosinca 2021.
Prihvaćeno 31. srpnja 2022.